National Park Service
U.S. Department of the Interior

Natural Resource Stewardship and Science

# Long-term Vegetation Change in Klondike Gold Rush National Historical Park

## *Using Historic Aerial Imagery to Detect Change in Forest and Shrubland Extent Along the Upper Chilkoot Trail*

Natural Resource Report NPS/KLGO/NRR—2017/1408

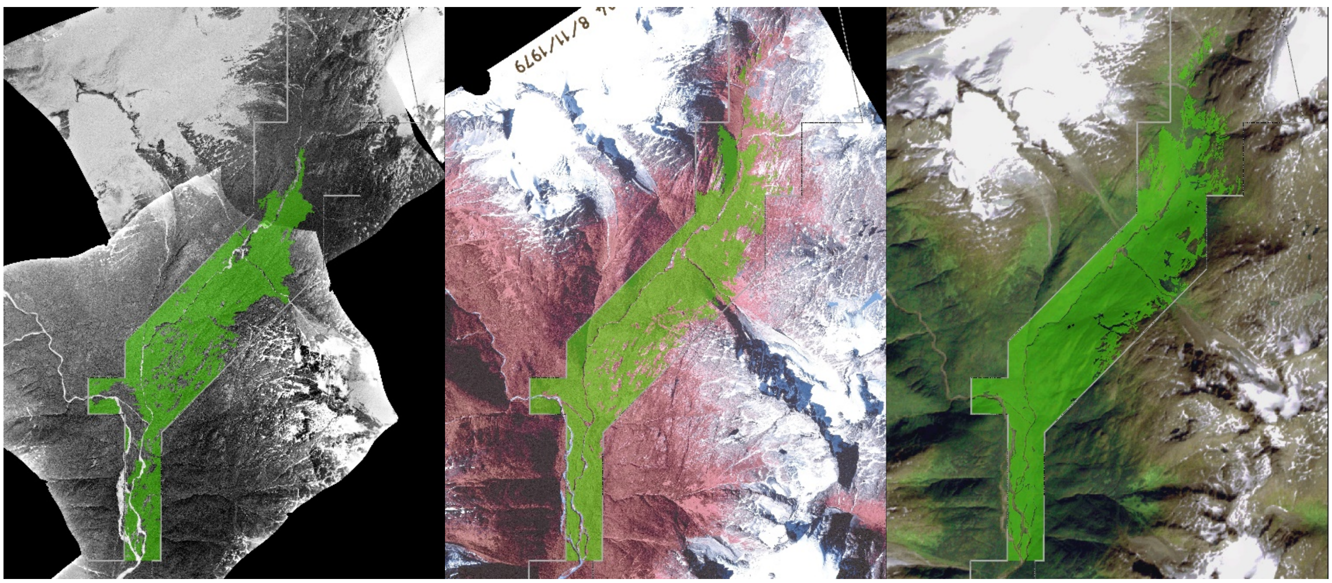

**ON THIS PAGE**
Photograph of Chilkoot Pass and lower trail corridor, Klondike Gold Rush National Historical Park, Alaska.

**ON THE COVER**
Extents of forest overlain on aerial imagery captured in 1948, 1979, and 2003/2005 within the upper Chilkoot Unit of Klondike Gold Rush National Historical Park.

All images courtesy of the National Park Service.

# Vegetation Change in Klondike Gold Rush National Historical Park

*Using historic aerial imagery to detect change in forest and shrubland extent along the upper Chilkoot Trail*

Natural Resource Report NPS/KLGO/NRR—2017/1408

Lindsey Flagstad and Tina Boucher

Alaska Center for Conservation Science
University of Alaska Anchorage
3211 Providence Dr.
Anchorage, Alaska 99508

March 2017

U.S. Department of the Interior
National Park Service
Natural Resource Stewardship and Science
Fort Collins, Colorado

The National Park Service, Natural Resource Stewardship and Science office in Fort Collins, Colorado, publishes a range of reports that address natural resource topics. These reports are of interest and applicability to a broad audience in the National Park Service and others in natural resource management, including scientists, conservation and environmental constituencies, and the public.

The Natural Resource Report Series is used to disseminate comprehensive information and analysis about natural resources and related topics concerning lands managed by the National Park Service. The series supports the advancement of science, informed decision-making, and the achievement of the National Park Service mission. The series also provides a forum for presenting more lengthy results that may not be accepted by publications with page limitations.

All manuscripts in the series receive the appropriate level of peer review to ensure that the information is scientifically credible, technically accurate, appropriately written for the intended audience, and designed and published in a professional manner. This report received informal peer review by subject-matter experts who were not directly involved in the collection, analysis, or reporting of the data.



This report is available in digital format from Natural Resource Publications Management website. To receive this report in a format that is optimized to be accessible using screen readers for the visually or cognitively impaired, please email irma@nps.gov**.**

Please cite this publication as:

Flagstad, L. and T. Boucher. 2017. Vegetation change in Klondike Gold Rush National Historical Park: Using historic aerial imagery to detect change in forest and shrubland extent along the upper Chilkoot Trail. Natural Resource Report NPS/KLGO/NRR—2017/1408. National Park Service, Fort Collins, Colorado.

NPS 461/137324, March 2017

# Contents

# Figures

# Tables

# Abstract

As climate exerts primary control on the broad-scale distribution and abundance of plant species, change in climate can elicit a delayed but commensurate response in vegetation. This project assesses change in the distribution of forest and shrubland over a 60-year period in the upper Chilkoot Unit of Klondike Gold Rush National Historical Park (NHP), Alaska. Here we document the magnitude and direction of this change by comparing the total areas of forest and shrubland as well as the positions of elevational treeline and shrubline on remotely-sensed imagery captured in 1948, 1979 and 2003/2005. This geospatial analysis shows clear increase in forest extent, presumably at the expense of shrubland as well as a greater annual rate of elevational treeline advance relative to shrubline. We interpret the greater shift in forest distribution as a successional response to gold rush-era disturbance that is compounded by niche expansion due to a warming climate.

## Acknowledgments

We would like to thank Emily Himmelstoss with the U.S. Geological Survey Coastal and Marine Geology Program for her generous technical support, Megumi Aisu with the Alaska Center for Conservation Science for her assistance with the orthorectification of historical imagery, and Paul Burger with the Alaska Regional Office of the National Park Service for financial support of this project.

## Introduction

Klondike Gold Rush National Historical Park (NHP) protects significant cultural and natural resources. The park commemorates the 1897-1898 passage of fortune-seekers through Chilkoot and White Passes inland to the Klondike goldfields near Dawson City (Ferreira 2011). These low-lying passes transect the rugged Coast Mountain Range and connect the coastal lowlands of southeast Alaska to the uplands of the Canadian interior. The rare mixing of maritime and continental climates across these passes results in both a rich flora and unusual species combinations (Nowacki et al. 2000).

This project assesses historic change in the distribution of forest and shrubland in the upper Chilkoot Unit of Klondike Gold Rush NHP. The Chilkoot Unit occupies 9,899 ha at the head of Lynn Canal where it rises from sea level to over 1,675 m along the Taiya River. Vegetation along the upper Taiya River transitions from boreal to alpine types along a steep ecological gradient. *Populus balsamifera* ssp. *trichocarpa* (black cottonwood) and *Picea sitchensis* (Sitka spruce) codominate valley floor floodplains. Above active floodplains, *Tsuga heterophylla* (western hemlock), a characteristic species of temperate rainforests, becomes increasingly dominant in mountain toe and sideslope forests, with this dominance transitioning to *Tsuga mertensiana* (mountain hemlock) in the subalpine. Tree species with greater affinity to interior climates such as *Betula papyrifera* (paper birch), *Pinus contorta* var. *latifolia* (lodgepole pine) and *Abies lasiocarpa* (subalpine fir) are found in more xeric and exposed sites of the hemlock-dominated forests. *Alnus viridis* ssp. *sinuata* (Sitka alder) shrublands develop in early-seral sites exposed by deglaciation or disturbed by avalanche, landslide, or flooding. In the subalpine, dwarf stands codominated by *Tsuga mertensiana* and *Abies lasiocarpa* grow interspersed with dwarf shrub and alpine meadow communities. With increasing exposure, alpine vegetation grades from dwarf ericaceous shrub to dry lichen-graminoid communities. Barren rock and perennial snow and ice occupy the highest, most exposed alpine areas.

Here we document the magnitude and direction of this change by comparing the position of elevational treeline and shrubline over the last 60 years on remotely-sensed imagery captured in 1948, 1979 and 2003/2005 in a GIS environment. This effort leverages a vegetation inventory recently completed for Klondike Gold Rush NHP by extracting the current distribution of forest and shrubland from the landcover map produced as part of the project (Flagstad and Boucher 2015). The historic distribution of forest and shrubland was manually-digitized on orthorectified, remotely-sensed imagery from both 1948 and 1979. The trend of vegetation resources was assessed by calculating areas of forest and shrubland occupancy for each image set as well as the rate of tree and shrubline position change over the 60-year period.

## Methods

Three sets of remotely-sensed imagery captured in 1948, 1979, 2003/2005 were selected to infer change in distribution of major vegetation types at 30 year intervals over an approximately 60-year time span within the upper Chilkoot Unit of Klondike Gold Rush NHP. Extent of forest and shrubland was manually digitized on each of these image sets and from this delineation, change in total area as well as the elevational limits of forest and shrubland were calculated. All geospatial work was completed in ArcGIS 10.4.1 using a Universal Transverse Mercator projection for Zone 8 North and referencing the North American Datum of 1983 (NAD_1983_UTM_Zone_8N).

### Image Selection

True-color aerial photography dating from July 6 -11, 1948 (U.S. Navy BAR00 project, 1:20,000, pixel size 1.15 m) and color-infrared satellite imagery captured August 11, 1979 (Alaska High-Altitude Photography, 1:60,000, pixel size 2.25 m) were selected to represent the historic distribution of vegetation in the Chilkoot Unit. The current (i.e. mid 2000s) extent of forest and shrubland was extracted from a landcover map recently completed for Klondike Gold Rush National Historical Park (Flagstad and Boucher 2015). This landcover project delineated 57 classes on a combination of both aerial photography and satellite imagery. For the Chilkoot Unit, both an orthorectified mosaic of aerial photographs taken on July 1, 2003 at a scale of 1:2,000 and pixel size of 0.15 m and an orthorectified satellite scene captured by the IKONOS-2 satellite on August 12, 2005 at a scale of 1:12,000 and pixel size of 2.27 m were used. The higher-resolution aerial photography, which was centered on the Chilkoot Trail corridor was used preferentially over the lower-resolution satellite imagery; see Figure 1 for the coverage areas of the 2003 and 2005 image sets.

While not used in analysis, imagery captured by the LANDSAT satellite on August 1, 1999 at a scale of 1:80,000 and pixel size of 30 m.  This natural color image was used as a background for many of the figures in this report as coverage for the park area is complete.

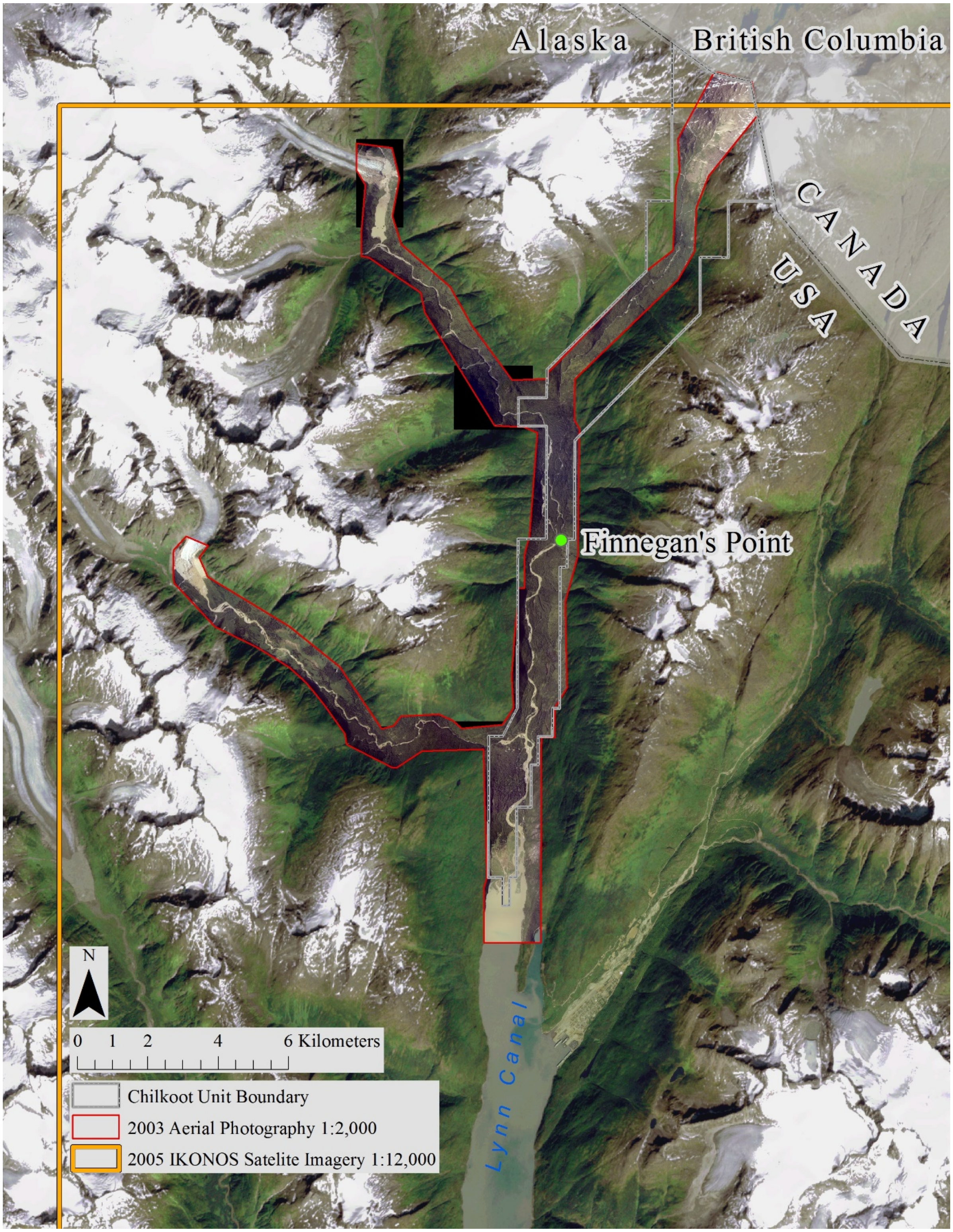


**Figure 1.** Coverages of remotely-sensed imagery representing the current extent of vegetation in the Chilkoot Unit of Klondike Gold Rush National Historical Park. The southern limit of vegetation delineation on historic imagery at Finnegan's Point is also shown. Background imagery was collected by the LANDSAT satellite on August 1, 1999.

## Historic Image Preparation

Aerial imagery captured in 1948 and 1979 were used to infer historic extent of forest and shrubland. The four aerial photographs dating from 1948 were scanned at 96 dpi (northernmost three images) and 72 dpi (southernmost image) for use. The two satellite images captured in 1979 were used in their native digital format 300 dpi (northernmost image) and 96 dpi (southernmost image). Georeferencing of the 1948 and 1979 images was completed with the addition of control points based on the IKONOS-2 2005 satellite imagery and the SDMI Best Data Layer (UAF-GINA 2016). Once these images were adequately positioned, distortion was corrected using the spline tool available through the ESRI ArcGIS raster georeferencing tool bar. The multiple images for each year were combined to single 1948 and 1979 images using the Mosaic to New Raster tool. The final georeferenced and mosaicked images used to infer vegetation patterns are shown in Figure 2.

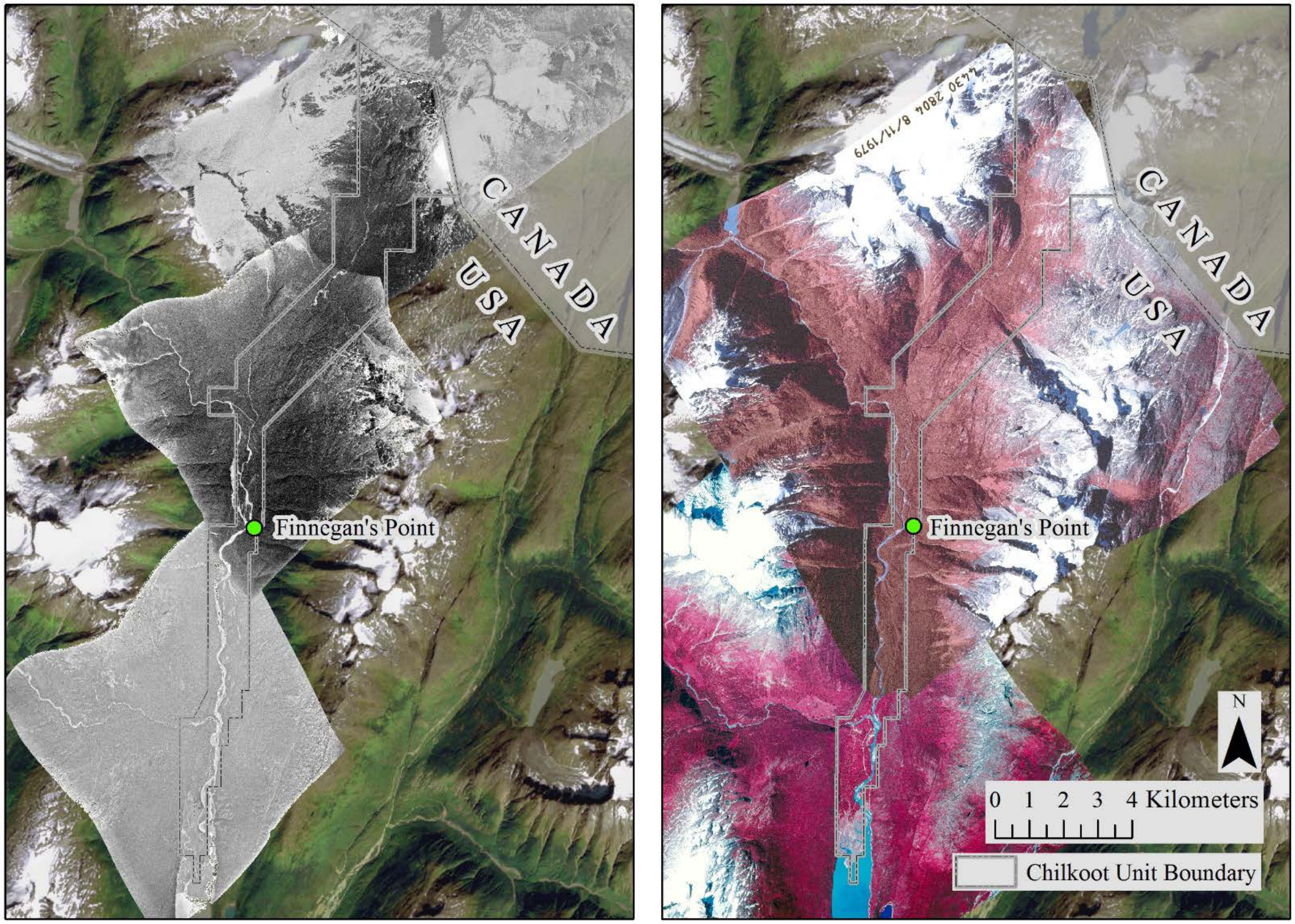


**Figure 2.** Final georeferenced and mosaicked images for 1948 (left) and 1979 (right). Background imagery was collected by the LANDSAT satellite on August 1, 1999.

## Digitization of Vegetation Boundaries

The historic extent of forest and shrubland was manually delineated on remotely-sensed imagery with reference to general patterns of image tone, texture, color, and contrast as well as historical ground-based photography (Figure 3). Polygons corresponding to the extent of forest and shrubland in 1948 and 1979 were digitized for the northern portion of the Chilkoot Unit where climate is expected to have the greatest effect on the distribution of vegetation. Although the extent of forest and shrubland has been digitized for the entirety of the Chilkoot Unit on the 2003/2005 image set as part of a recently-completed landcover mapping project (see Flagstad and Boucher 2015), digitization on the 1948 and 1979 image sets was curtailed north of Finnegan's Point at the break in the park boundary corresponding to a Latitude of 59° 34' 43.5576" N (Figure 1). Vegetation was not digitized south of Finnegan's Point as elevational shrubline and treeline occur well above the Park boundary along the lower Chilkoot Trail corridor. The lead author for the landcover mapping project (Flagstad and Boucher 2015) and this report was responsible for delineating vegetation on all image sets. While the manual digitization of landcover types is undoubtedly a subjective process, consistency is gained from having the same person delineating.

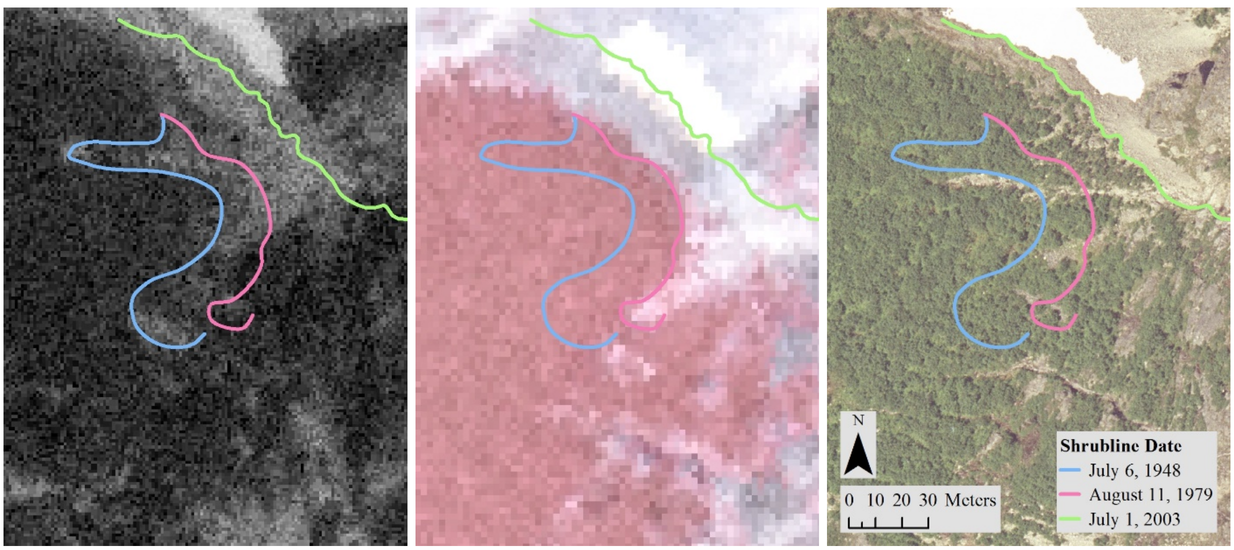


**Figure 3.** Example digitization of shrubline position on 1948 (left), 1979 (middle), and 2003 (right) imagery.

Approximately 20 ground-based photo pairs, comprised of one photograph dating from the gold rush era (1890-1910) and a current (2013/2014) image captured from the same location and field of view were made available by the National Park Service for reference (Karpilo and Venator 2015; Figure 4). While these photo pairs were highly informative towards general patterns of succession, the time span between the older member of each pair and the 1948 aerial imagery encompassed too much successional change to allow the gold rush era images to be used for ground truthing the 1948 imagery.

**Figure 4.** Example of repeat photography captured by Karpilo and Venator (2015). Historic (1897, Frank LaRoche) and current (August 18, 2013 R.D. Karpilo Jr. and S.C. Venator) images of the Taiya River Valley taken from Trail Camp looking south towards Dyea.

For the purposes of this project, treeline is considered the elevational extent of full stature (not dwarf), erect (not krummholz) trees comprising open to closed canopy forests (greater than 25% canopy cover). Similarly, shrubline is considered the elevational extent of open to closed (greater than 25% canopy cover) shrubs greater than 20 cm tall (i.e. not dwarf). Patches of vegetation occupying less than 1 ha were not delineated, similarly 'donuts' less than 1 ha within larger shrub or tree stands were not delineated. Sections of tree or shrubline that are constrained by episodic disturbance events (e.g. land or snowslides, seasonal river or periodic glacial outburst flooding) or topography (e.g. bedrock-constrained river channels, mountainside cliffs), which restricts response to climate change were delineated but not evaluated for vegetation boundary change. Vegetation boundaries within terrain shadows, which were prevalent in both the 1948 and 1979 image sets were delineated however the high uncertainty associated with these boundary positions disqualified these line segments from rate-of-change analysis.

Change in total area of forest and shrubland was calculated by summing the area of polygons by vegetation type (forest or shrub) or each year. Development of a forest extent from the 2015 landcover map required selecting all polygons attributed as an open or closed forest type and then dissolving these types to a multipart forest polygon. Similarly, development of a shrubland extent required selecting all polygons attributed as a low or tall shrub type and then dissolving these types to a multipart shrub polygon.

Change in treeline and shrubline position were quantified using the Digital Shoreline Analysis System (DSAS; Thieler et al. 2009). DSAS is ArcGIS extension developed by the National Oceanic and Atmospheric Administration (NOAA) that computes rate-of-change statistics from multiple historic boundary positions. Although this software was originally developed for coastal applications (e.g. Gibbs and Richmond 2015), DSAS is can be applied to any boundary-change problem incorporating a clearly-identified feature position at discrete times, such as landcover boundaries (e.g. Sharma et al. 2016).

Rate-of-change statistics were only calculated where vegetation boundaries were not affected by episodic disturbance or curtailed by topography, could be visualized with acceptable uncertainty for all three image sets, and were generally aligned (i.e. not exceedingly crenulated and/or overlapping). Because rates of change are based on measured differences between vegetation boundaries through time, each vegetation line was attributed with a date and measure of uncertainty. Uncertainty was assigned to lines in accordance with the resolution of the imagery. Specifically, default uncertainty values were calculated as twice the hypotenuse of their ground pixel dimension, which represents the maximum displacement possible for a point from its true location within a given pixel (Table 1). It is important to note that the measures of uncertainty given here should be considered a minimum value as they are easily compounded by orthorectification and georeferencing errors as well as the misinterpretation of types by the delineator.

**Table 1.** Estimates of uncertainty for the remotely-sensed image sets used to assess vegetation change.

| Image Date | Pixel Dimension | Uncertainty (m) |
|---|---:|---:|
| July 6, 1948 | 1.15 | 3.25 |
| August 11, 1979 | 2.27 | 6.42 |
| July 1, 2003 | 0.15 | 0.42 |
| August 12, 2005 | 1 | 2.83 |

Distance between vegetation lines are measured along a series of transects, which are cast at a user-defined interval from a baseline. Baselines were developed for this project by buffering selected vegetation lines by 20 m and then tracing the downgradient portion of the resulting polygon. Where this approach yielded an exceedingly convoluted baseline and thus intersecting transects, we instead constructed an arced segment, positioned approximately 20 m downgradient from the lowest elevation vegetation boundary. The baselines were then used by the DSAS software to cast transects upgradient through the vegetation boundaries (Figure 5). Transect length was assigned by estimating the maximum distance between the baseline and highest elevation vegetation boundary. Transects were cast upgradient every 20 m along the baseline and were manually edited so that they intersected all three vegetation boundaries and were approximately orthogonal to these boundaries.

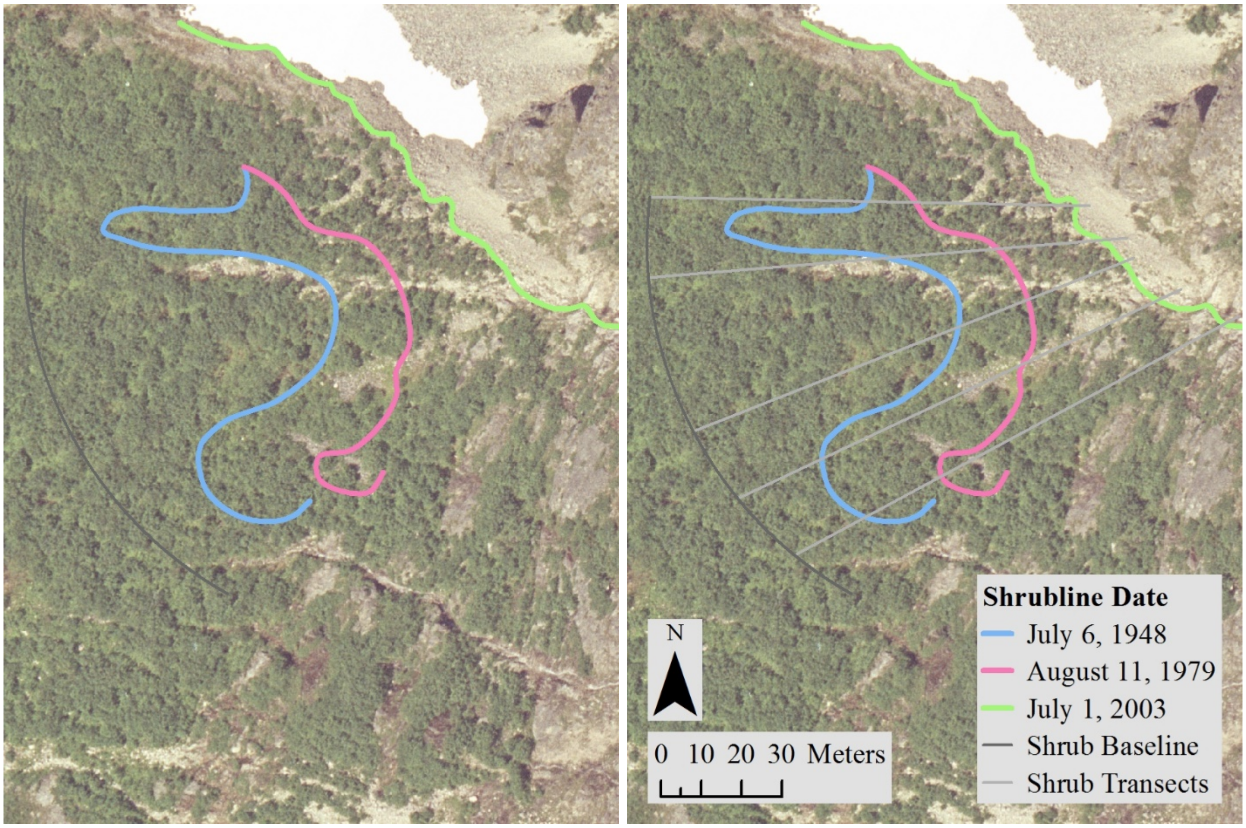


**Figure 5.** Example construction of baseline and the casting of transects using the DSAS software program. Background imagery is the orthorectified mosaic of aerial photographs taken on July 1, 2003.

Transects that intersected other transects or failed to intersect all three vegetation boundaries were either trimmed, repositioned, or deleted. Transects were trimmed to prevent intersection among exceedingly long transects and/or to avoid multiple intersections with the same vegetation boundary. Transects were repositioned to ensure intersection with all three vegetation boundaries; movement of the transect from its original position was limited to within 5 m of its origin along the baseline and/or within $10^{o}$ of its original aspect. If an intersection with the vegetation boundaries could not be achieved within these parameters, the transect was deleted. A linear regression rate with confidence interval of 90% was used to calculate the annual rate of vegetation boundary change. A linear regression rate-of-change statistic is determined from the slope of the least-squares regression line that minimizes the sum of the squared residuals among the vegetation lines for a transect (Himmelstoss 2009).

## Results

Change in the distribution of shrubland and forest types is both present and detectable in the upper Chilkoot Unit of Klondike Gold Rush NHP. Change in area was summed by vegetation type for each image set (Table 2). Forested area increased with time (Figure 6), however shrub area decreased from 1948 to 1979 and increased slightly from 1979 to the mid-2000s (Figure 7).

**Table 2.** Absolute change in forest and shrubland area as calculated from manual delineation of extents on historic aerial imagery.

| Image Year | Forest Area ($km^2$) | Shrub Area ($km^2$) |
|---|---:|---:|
| 1948 | 9.39 | 3.93 |
| 1979 | 12.74 | 1.48 |
| 2003, 2005 | 14.63 | 1.97 |

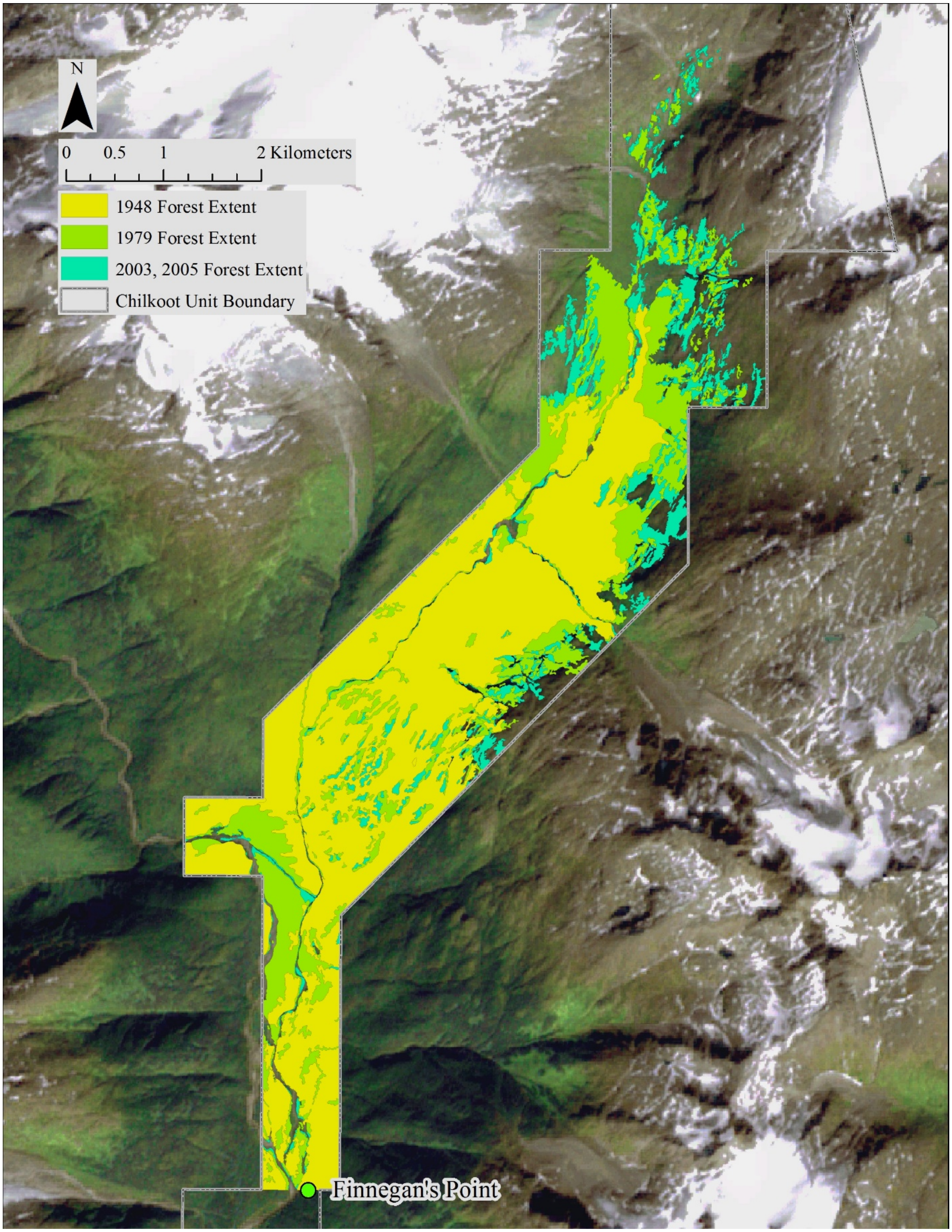


**Figure 6.** Relative change in forested extent among dated image sets in the upper Chilkoot Unit, Klondike Gold Rush NHP, Alaska. Background imagery was collected by the LANDSAT satellite on August 1, 1999.

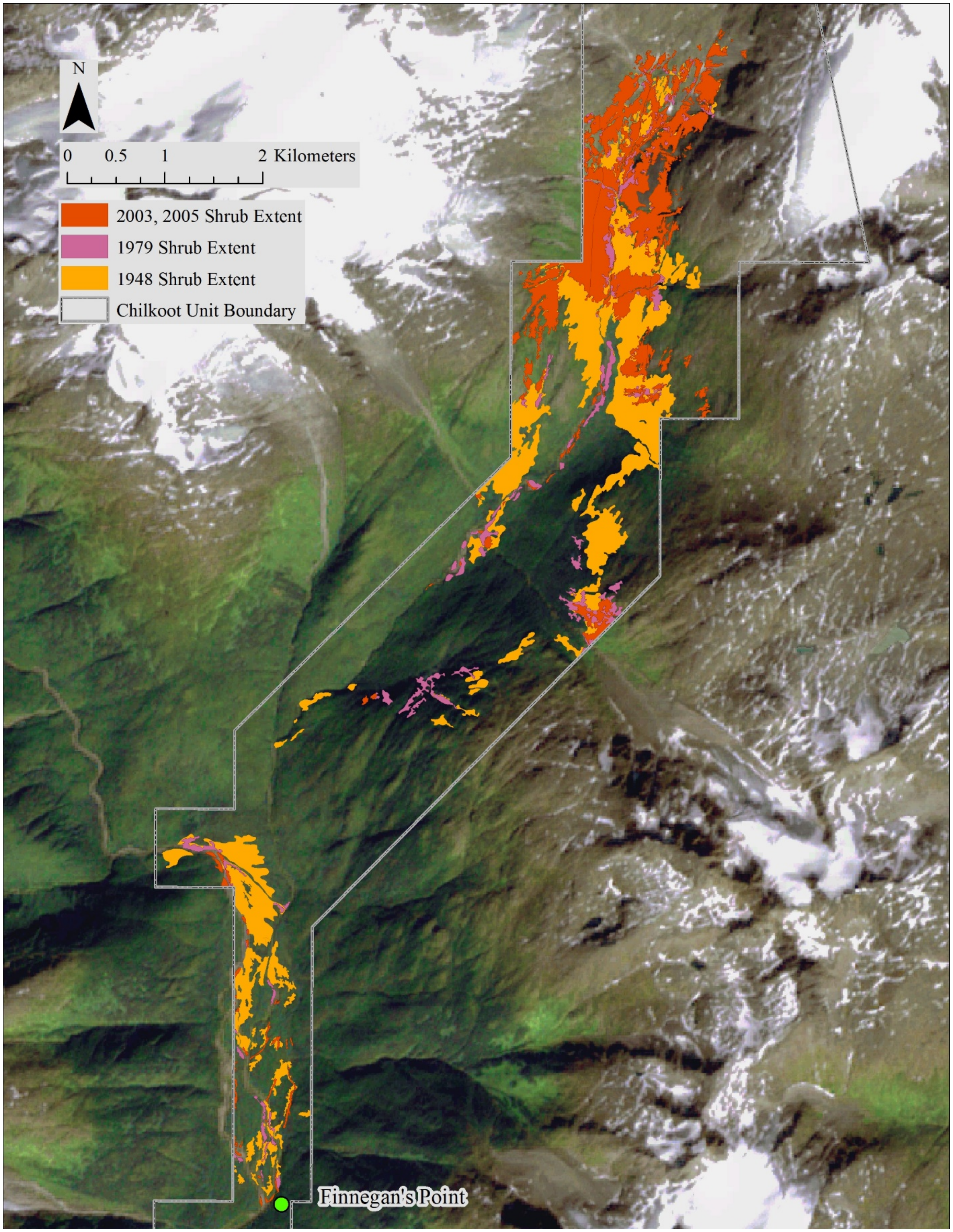


**Figure 7.** Relative change in shrubland extent among dated image sets in the upper Chilkoot Unit, Klondike Gold Rush NHP, Alaska. Background imagery was collected by the LANDSAT satellite on August 1, 1999.

A total of 10 shrubline and 7 treeline groups were assessed for boundary change (Figure 8); 62 and 51 transects were cast along 1,204 m of shrub baseline and 2,313 m of tree baseline, respectively. Average annual rate of treeline change was calculated as 3.5 m/y ±5.1 m. Average annual rate of shrubline change was calculated as 0.66 m/y ±1.2 m. Annual fluctuation is large, as indicated by the confidence intervals, which are approximately double the average rate of change for both tree and shrubline. While rates for both forest and shrubline show high spatial variation both among and within transect groups, rates are consistently higher towards the head of the pass (Figure 9 and Figure 10).

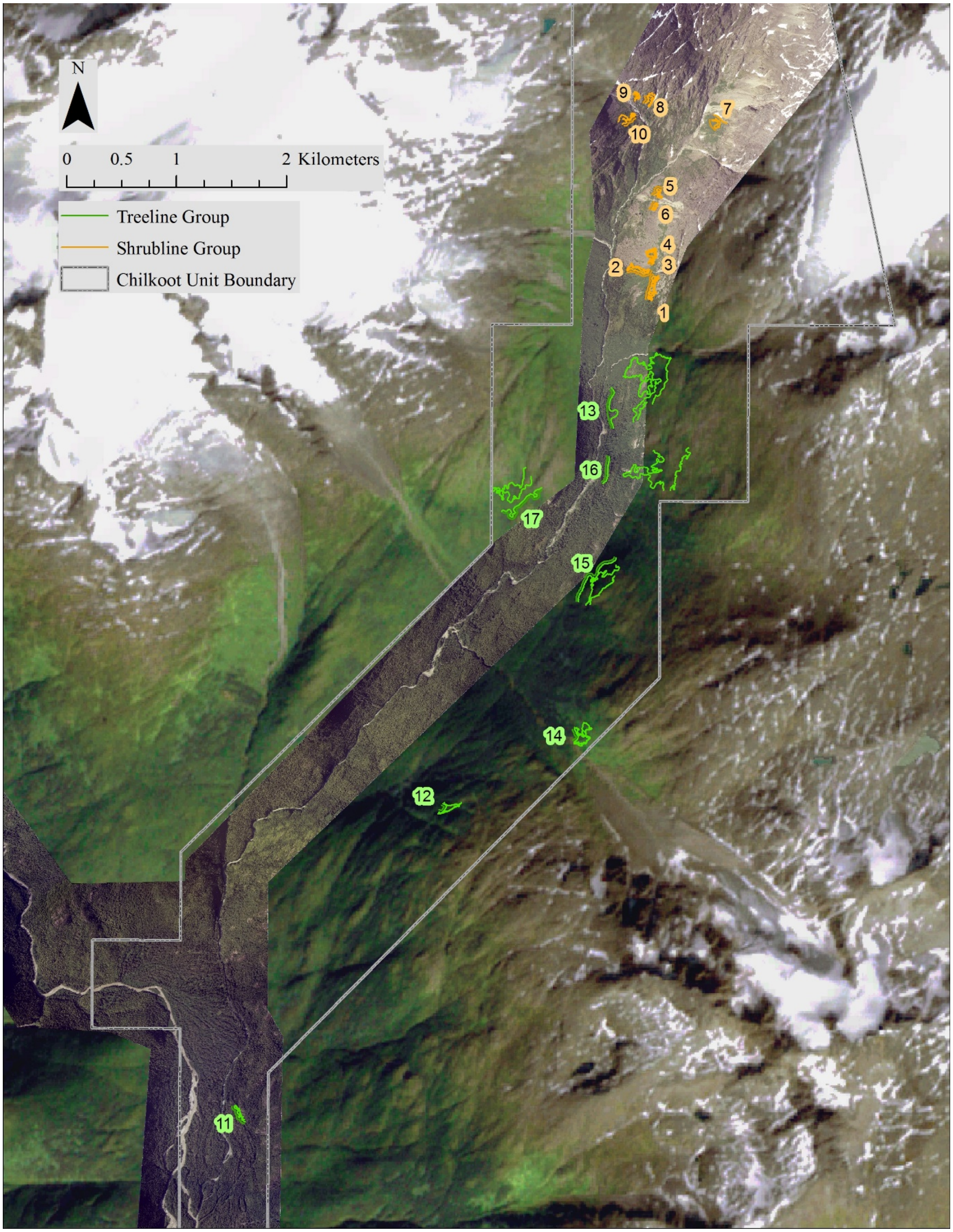


**Figure 8.** Location of shrubline (labels 1-10) and treeline (labels 11-17) groups advanced for assessment of vegetation boundary change, upper Chilkoot Trail Unit, Alaska. Aerial photography is the orthorectified mosaic taken on July 1, 2003; background imagery was collected by the LANDSAT satellite on August 1, 1999.

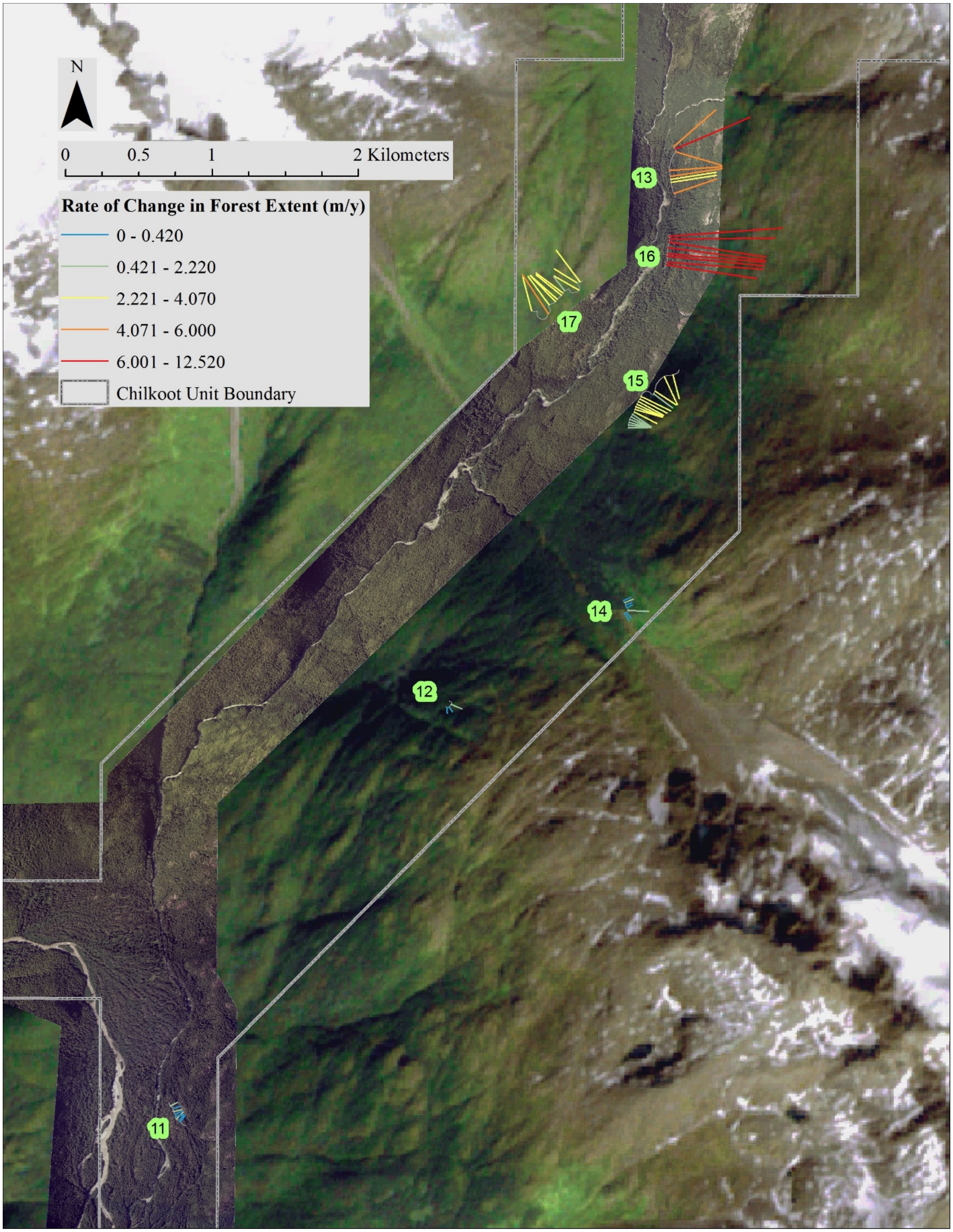


**Figure 9.** Annual rates of change (m/y) in treeline calculated from historic vegetation boundary positions, upper Chilkoot Pass, Alaska. Aerial photography is the orthorectified mosaic taken on July 1, 2003; background imagery was collected by the LANDSAT satellite on August 1, 1999.

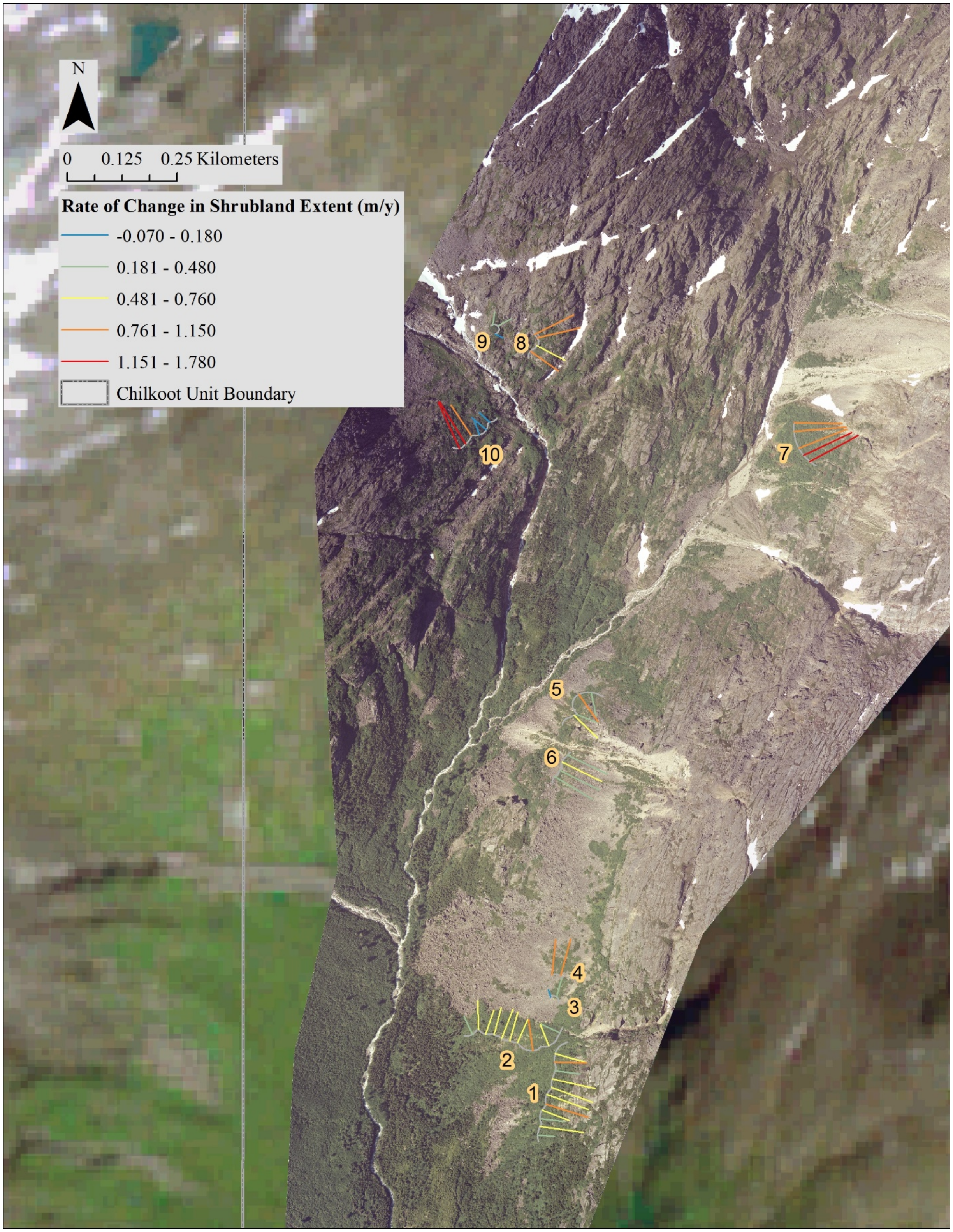


**Figure 10.** Annual rates of change (m/y) in shrubline calculated from historic vegetation boundary positions, upper Chilkoot Pass, Alaska. Aerial photography is the orthorectified mosaic taken on July 1, 2003; background imagery was collected by the LANDSAT satellite on August 1, 1999.

# Discussion

As climate exerts primary control on the broad-scale distribution and abundance of plant species, change in climate can elicit a delayed but commensurate response in vegetation. In the upper Chilkoot Unit of Klondike Gold Rush NHP, change in the distribution of shrubland and forest types is both evident to the on-the-ground observer as well as detectable in a geospatial environment. A recently completed evaluation of gold rush-era ground photos to current environmental condition notes, among other changes in park resources: glacial recession, vegetative succession, changes in ecosystem composition and connectivity, vertical advance of treeline, and increase in vegetation density (Karpilo and Venator 2015). The geospatial analysis presented here provide quantitative support for these findings. Specifically, the total area of forest is shown to increase over the period of analysis, apparently at the expense of shrubland and similarly, treeline advance is shown to significantly outpace shrubline advance.

The expansion of forest relative to shrubland, which shows a net decrease in total area over the 60-year period, is interpreted to be a result of natural succession following gold-rush-era disturbance. The Klondike region, particularly the Taiya River corridor and Chilkoot Pass, was highly disturbed at the turn of the nineteenth century. Forests were cleared; settlements erected, and mechanized transport built to move 30,000 gold seekers, animals, and goods through the pass during the winter of 1897-1898. Logging and fire left much of the Taiya River corridor and headwaters bereft of forested vegetation and stripped to mineral soil in some areas (Ferreira 2011). These are the disturbed conditions to which deciduous shrubs with ruderal life history traits are highly adapted. Ability to fix nitrogen (*Alnus* species), withstand sedimentation through suckering and coppice sprouting (*Salix* species), and grow quickly (*Alnus* and *Salix* species) likely explains the abundance of these shrubs in the 1948 imagery.

In the absence of continued disturbance, similar landscapes in southeast Alaska have been shown to achieve peak shrub biomass 15-25 years post-disturbance and forest canopy closure 25-35 years post disturbance (Alaback 1982, DeMeo et al. 1992). The development of canopy gaps and subsequent initiation of secondary successional processes is thought to begin 140-160 years post-disturbance. Ultimately these forests mature to old-growth types dominated by *Tsuga heterophylla* and characterized by trees exceeding ages of 250 years, a multilayered canopy, and presence of snags and coarse woody debris (Alaback 1982, DeMeo et al. 1992). Assuming these successional intervals are applicable to the Klondike region, in 1948, shrublands in the upper Chilkoot Unit had likely achieved their maximum extent and were beginning to be colonized by coniferous tree species. By 1979, forests were well-established with closed canopies and in the mid-2000s, over one hundred years post-disturbance, forests flanking the Chilkoot Trail are in a phase of maximum canopy closure in advance of gap succession.

Different from shifts in total areas of forest and shrubland, which in the upper Chilkoot Unit are chiefly attributed to natural succession, the upward movement of elevational tree and shrubline is largely interpreted as response to a warming climate. Climate change in the Klondike region is evidenced by the recession of glaciers following a period of colder temperatures and glacial advance during the Little Ice Age (circa 1850 AD). Both gold-rush-era ground photography and the 1948 aerial imagery show permanent ice and snow within the Chilkoot Unit boundaries; however, in the last half century this presence has diminished in concert with thinning and recession of mountain glaciers across Alaska (Arendt et al. 2002, KellerLynn 2009).

Increased growth of vegetation is a widely-documented response to a warming climate both globally (Nemani et al. 2003) and regionally (Jorgenson et al. 2006). At the local scale, decreasing glacial extent in the Chilkoot Unit provides new substrates and ameliorates conditions for plant growth. While numerous Alaska-based studies have linked shrubline expansion to increased summer temperatures (Tape et al. 2006, Verbyla 2008), the trend of forests is less clear with recent studies showing divergent responses in growth rates at treeline (Ellison 2015, Lloyd 2005). Additionally, a comparison of tree and shrubline change in the southcentral Alaska, which was similarly based on the interpretation of remotely-sensed imagery returned rates contradictory to those calculated for the Chilkoot Pass (Dial et al. 2015). While treeline advance in the upper Chilkoot Unit is over five times the rate calculated for shrubline, shrub expansion outpaced forest expansion at sites in the Chugach and Kenai Mountains during the period of analysis (1972-2012), a difference that is attributed in part to a successional lag of tree establishment relative to more easily dispersed, fast-growing shrubs (Dial et al. 2015). Although the rates of treeline advance are, shown herein are seemingly contradictory to the results returned for southcentral, they may also be interpreted in a successional context. We propose that the faster rate of forest expansion, at the expense of shrubland is because shrubs have reached their successional maximum (i.e. realized niche is approaching fundamental niche) and are currently responding more slowly to climatic drivers whereas forests have not yet reached their successional maximum (i.e. realized niche does not yet approximate fundamental niche), and thus are responding to the compound forces of succession and climate.

In the upper Chilkoot Unit annual rates of tree and shrubline change are not uniform across the landscape. Higher rates of advance were returned for segments at the head of the Taiya River Valley on comparatively gentle subalpine slopes with southwest aspect. It is suspected that higher rates of tree and shrubline advance in this area may relate to differences in microtopography among these and other mountain sideslopes (Malanson et al. 2007). While we cannot prove causality, a greater availability germination sites, fewer topographic barriers to dispersal, and/or greater solar radiation may promote the elevational expansion of trees and shrubs on these less rugged and presumably warmer slopes (Hille Ris Lambers et al. 2013).

On the Alaska side of Chilkoot Pass December is the coldest month with an average ambient air temperature of $11.3^{o}$F ($-11.5^{o}$C; 2014) while average monthly temperature peaks at $43.2^{o}$F ($6.2^{o}$C; 2015) in August (Chilkoot Pass RAWS Station, WRCC 2016[1]). As the Klondike region is projected to become warmer over the next century, with winter maximum temperatures forecast to transition above freezing (Schirokauer 2009) it is likely that gains in forest area and elevational position will continue. Conversion of shrubland to forest and treeline advance in the upper Chilkoot Pass appears

1 Weather station data highly-discontinuous; December 2014 air temperature averaged from two records.

to be driven by natural succession and sped by a warming climate. In the absence of future landscape-scale disturbance, it is likely that forests will continue to expand and mature, eventually affecting the alpine nature of the park with long-term implications for both abiotic and linked biotic processes.

## Literature Cited

Alaback, P.B. 1982. Dynamics of understory biomass in Sitka spruce-western hemlock forests of southeast Alaska. Ecology 63:1932-1948.

Arendt, A.A., K.A. Echelmeyer, W.D. Harrison, C.S. Lingle, V.B. Valentine. 2002. Rapid Wastage of Alaska Glaciers and Their Contribution to Rising Sea Level. Science 297:382-386.

Deal, R.L., P.E. Hennon, E.H. Orlikowska, and D.V. D‘Amore. 2004. Stand dynamics of mixed red alder–conifer forests of southeast Alaska. Canadian Journal of Forest Research 34: 969-980.

Dial, R.J., T.S. Smeltz, P.F. Sullivan, C.L. Rinas, K. Timm, J.E. Geck, S.C. Tobin, T.S. Golden and E.C. Berg. 2015. Shrub-line but not treeline advance matches climate velocity in montane ecosystems of south-central Alaska. Global change biology. 22: 1841–1856.

DeMeo, T., J. Martin, and R.A. West. 1992. Forest plant association management guide, Ketchikan Area, Tongass National Forest. R10-MB-210. USDA Forest Service Alaska Region. Juneau, Alaska.

Ellison, S.B.Z., 2015. Can divergent white spruce growth in the eastern Brooks Range be explained by low soil nutrient availability? (Doctoral dissertation, UNIVERSITY OF ALASKA ANCHORAGE).

Ferreira, S.L. 2011. The Chilkoot Trail - Cultural Landscape Report for the Chilkoot Trail Historic Corridor. Part 1: History, Existing Conditions, & Analysis. Produced by the Cultural Landscapes Program, Alaska, in cooperation with Klondike Gold Rush National Historical Park. 407 pp.

Flagstad, L. and T. Boucher. 2015. Klondike Gold Rush National Historical Park; Landcover classes and plant associations. Natural Resource Report NPS/KLGO/NRR—2015/917. National Park Service, Fort Collins, Colorado.

Gibbs, A.E. and B.M. Richmond, 2015. National assessment of shoreline change—Historical shoreline change along the north coast of Alaska, US–Canadian border to Icy Cape. US Geological Survey Open-File Report, 1048, p.96.

Hille Ris Lambers, J., M.A. Harsch, A.K. Ettinger, K.R. Ford, and E.J. Theobald. 2013. How will biotic interactions influence climate change–induced range shifts? Annals of the New York Academy of Sciences, 1297(1), pp.112-125.

Himmelstoss, E.A. 2009. “DSAS 4.0 Installation Instructions and User Guide” in: Thieler, E.R., Himmelstoss, E.A., Zichichi, J.L., and Ergul, Ayhan. 2009 Digital Shoreline Analysis System (DSAS) version 4.0 — An ArcGIS extension for calculating shoreline change: U.S. Geological Survey Open-File Report 2008-1278.

Jorgenson, M. Torre, Gerald V. Frost, Will E. Lentz, and Alan J. Bennett. 2006. Photographic monitoring of landscape change in the southwest Alaska network of national parklands. Report

No. NPS/AKRSWAN/NRTR-2006/03. ABR, Inc.–Environmental Research & Services, Fairbanks, Alaska.

Karpilo, R.D. Jr., S. C. Venator, Documenting over a century of natural resource change with repeat photography in Klondike Gold Rush National Historical Park, Alaska. Natural Resource Report NPS/KLGO/NRR—2015/1017. National Park Service, Fort Collins, Colorado.

KellerLynn, K. 2009. Geologic Resources Inventory Scoping Summary, Klondike Gold Rush National Historical Park, Alaska. Produced by, Geologic Resources Division, National Park Service. 17 pp.

Lloyd, A.H., 2005. Ecological histories from Alaskan tree lines provide insight into future change. Ecology, 86(7), pp.1687-1695.

Malanson, G.P., D.R. Butler, D.B. Fagre, S.J. Walsh, D.F. Tomback, L.D. Daniels, L.M. Resler, W.K. Smith, D.J. Weiss, D.L. Peterson, and A.G. Bunn, 2007. Alpine treeline of western North America: linking organism-to-landscape dynamics. Physical Geography, 28(5), pp.378-396.

Nemani, R.R., Keeling, C.D., Hashimoto, H., Jolly, W.M., Piper, S.C., Tucker, C.J., Myneni, R.B. and Running, S.W., 2003. Climate-driven increases in global terrestrial net primary production from 1982 to 1999. science, 300(5625), pp.1560-1563.

Nowacki, G., P. Spencer, T. Brock, M. Fleming, and T. Jorgenson. 2000. Narrative descriptions for the ecoregions of Alaska and neighboring territories. Unpublished report.

Sharma, S., J. Goff, R.M. Moody, A. McDonald, D. Byron, K.L. Heck Jr, S.P. Powers, C. Ferraro, and J. Cebrian. 2016. Effects of Shoreline Dynamics on Saltmarsh Vegetation. PloS one 11, no. 7 e0159814.

Schirokauer, D. 2009. Klondike Gold Rush National Historical Park, Skagway, Alaska. Natural Resources Program Summary Report. 15 pp.

Tape, K., M. Sturm, and C. Racine. 2006. The evidence for shrub expansion in northern Alaska and the Pan-Arctic. Global Change Biology, 12(4), pp.686-702.

Thieler, E.R., Himmelstoss, E.A., Zichichi, J.L., and Ergul, Ayhan, 2009, Digital Shoreline Analysis System (DSAS) version 4.3— An ArcGIS extension for calculating shoreline change: U.S. Geological Survey Open-File Report 2008-1278.

UAF (University of Alaska Fairbanks)-GINA/SDMI http://alaskamapped.org/bdl Accessed July, 2016.

Verbyla, D., 2008. The greening and browning of Alaska based on 1982–2003 satellite data. Global Ecology and Biogeography, 17(4), pp.547-555.

Western Regional Climate Center (WRCC) 2016. Station data inventory web page. http://www.wrcc.dri.edu/ (accessed October 2016).

# Appendix A

Position, distance, and rate of change statistics for historic and current treelines in the upper Chilkoot Unit of Klondike Gold Rush NHP.

| Treeline Group | Transect ID | Start (UTM Easting) | Start (UTM Northing) | End (UTM Easting) | End (UTM Northing) | Azimuth (degrees) | Net Treeline Movement (m) | End Point Rate (m/y) | Confidence of Endpoint Rate (90%, m) | Linear Regression Rate (m/y) | Confidence of Linear Regression Rate (90%, m) |
|---|---|---|---|---|---|---|---|---|---|---|---|
| 11 | 191 | 481511.33 | 6607036.3 | 482414.64 | 6607465.3 | 64.6 | 25.53 | 0.46 | 0.06 | 0.47 | 0.476 |
| 11 | 192 | 481537.95 | 6607013.4 | 482467.15 | 6607383 | 68.31 | 15.04 | 0.27 | 0.06 | 0.28 | 0.54 |
| 11 | 193 | 481536.5 | 6606993.9 | 482504.97 | 6607243 | 75.57 | 25.65 | 0.47 | 0.06 | 0.48 | 1.186 |
| 11 | 194 | 481547.24 | 6606977.3 | 482475.86 | 6607348.3 | 68.22 | 18.31 | 0.33 | 0.06 | 0.33 | 0.148 |
| 11 | 195 | 481555.49 | 6606943.1 | 482270.95 | 6607641.7 | 45.68 | 32.51 | 0.59 | 0.06 | 0.6 | 0.761 |
| 11 | 196 | 481573.76 | 6606936.5 | 482182.36 | 6607730 | 37.49 | 0.89 | 0.02 | 0.06 | 0.02 | 0.267 |
| 11 | 197 | 481549.47 | 6606961.4 | 482521.68 | 6607195.5 | 76.46 | 21.13 | 0.38 | 0.06 | 0.39 | 0.662 |
| 11 | 198 | 481582.34 | 6606922.5 | 482298.48 | 6607620.4 | 45.74 | 7.47 | 0.14 | 0.06 | 0.16 | 1.701 |
| 12 | 154 | 483405.27 | 6609758.1 | 483443.59 | 6608758.8 | 177.8 | 2.95 | 0.05 | 0.075 | 0.05 | 0.142 |
| 12 | 155 | 483421.8 | 6609761.3 | 483970.58 | 6608925.3 | 146.72 | 11.23 | 0.2 | 0.075 | 0.2 | 0.612 |
| 12 | 156 | 483434.05 | 6609777 | 484359.97 | 6609399.3 | 112.19 | 40.78 | 0.71 | 0.075 | 0.73 | 2.324 |
| 13 | 62 | 484968.08 | 6613575.1 | 485888.66 | 6613965.6 | 67.01 | 517.29 | 9.06 | 0.075 | 9.04 | 1.893 |
| 13 | 210 | 484969.4 | 6613556.1 | 485929.54 | 6613276.5 | 106.23 | 289.23 | 5.26 | 0.06 | 5.41 | 12.83 |
| 13 | 215 | 484957.54 | 6613271.4 | 485894.1 | 6613621.9 | 69.48 | 257.34 | 4.68 | 0.06 | 4.79 | 9.247 |
| 13 | 216 | 484937.04 | 6613348 | 485925.58 | 6613498.9 | 81.32 | 218.99 | 3.98 | 0.06 | 4.07 | 6.856 |
| 13 | 217 | 484934.02 | 6613367.7 | 485922.56 | 6613518.7 | 81.32 | 205.89 | 3.74 | 0.06 | 3.79 | 3.798 |
| 13 | 218 | 484924.96 | 6613427.1 | 485922.48 | 6613497.6 | 85.96 | 322.6 | 5.87 | 0.06 | 6 | 10.835 |

| Treeline Group | Transect ID | Start (UTM Easting) | Start (UTM Northing) | End (UTM Easting) | End (UTM Northing) | Azimuth (degrees) | Net Treeline Movement (m) | End Point Rate (m/y) | Confidence of Endpoint Rate (90%, m) | Linear Regression Rate (m/y) | Confidence of Linear Regression Rate (90%, m) |
|---|---|---|---|---|---|---|---|---|---|---|---|
| 13 | 219 | 484931 | 6613387.5 | 485919.55 | 6613538.4 | 81.32 | 250.34 | 4.55 | 0.06 | 4.62 | 5.702 |
| 13 | 220 | 484955.14 | 6613589.7 | 485703.55 | 6614252.9 | 48.45 | 331.59 | 6.03 | 0.06 | 5.98 | 4.599 |
| 14 | 163 | 484610.78 | 6610491.6 | 485515.49 | 6610917.6 | 64.78 | 23.41 | 0.41 | 0.075 | 0.42 | 0.664 |
| 14 | 164 | 484619.24 | 6610473.6 | 485545.22 | 6610851.2 | 67.82 | 34.31 | 0.6 | 0.075 | 0.61 | 0.623 |
| 14 | 165 | 484625.57 | 6610455.3 | 485546.14 | 6610845.9 | 67.01 | 14.63 | 0.26 | 0.075 | 0.26 | 0.73 |
| 14 | 166 | 484634.5 | 6610437.7 | 485506.33 | 6610927.5 | 60.67 | 14.05 | 0.25 | 0.075 | 0.25 | 0.232 |
| 14 | 167 | 484644.34 | 6610421.9 | 485641.79 | 6610350.5 | 94.1 | 96.8 | 1.7 | 0.075 | 1.75 | 6.92 |
| 14 | 168 | 484614.84 | 6610397 | 485126.15 | 6609537.6 | 149.25 | 9.23 | 0.16 | 0.075 | 0.18 | 2.614 |
| 14 | 169 | 484632.27 | 6610406.5 | 485277.5 | 6609642.5 | 139.82 | 21.25 | 0.37 | 0.075 | 0.39 | 1.723 |
| 15 | 170 | 484645.34 | 6611667.6 | 485645.04 | 6611692.2 | 88.59 | 113.75 | 1.99 | 0.075 | 2.03 | 4.429 |
| 15 | 171 | 484644.67 | 6611687.4 | 485639.2 | 6611582.9 | 96 | 115.02 | 2.01 | 0.075 | 2.05 | 4.697 |
| 15 | 172 | 484649.45 | 6611706.8 | 485619.81 | 6611465.1 | 103.98 | 113.07 | 1.98 | 0.075 | 2.02 | 4.699 |
| 15 | 173 | 484654.29 | 6611726 | 485586.85 | 6611365 | 111.16 | 111.88 | 1.96 | 0.075 | 2 | 4.745 |
| 15 | 174 | 484663.61 | 6611743.3 | 485545.56 | 6611272 | 118.12 | 109.22 | 1.91 | 0.075 | 1.95 | 4.536 |
| 15 | 175 | 484672.86 | 6611760.8 | 485508.7 | 6611211.8 | 123.3 | 109.69 | 1.92 | 0.075 | 1.96 | 4.235 |
| 15 | 176 | 484685.03 | 6611776 | 485577.7 | 6611325.2 | 116.79 | 132.21 | 2.32 | 0.075 | 2.33 | 1.671 |
| 15 | 178 | 484690.09 | 6611794.9 | 485651.57 | 6611520 | 105.95 | 158.97 | 2.78 | 0.075 | 2.78 | 0.454 |
| 15 | 179 | 484695.67 | 6611813.2 | 485628.59 | 6611453.1 | 111.1 | 162.5 | 2.85 | 0.075 | 2.84 | 0.886 |
| 15 | 180 | 484704.13 | 6611831.3 | 485602.41 | 6611391.8 | 116.07 | 163.86 | 2.87 | 0.075 | 2.85 | 2.258 |
| 15 | 181 | 484713.23 | 6611849.1 | 485591.63 | 6611371.1 | 118.55 | 167.22 | 2.93 | 0.075 | 2.89 | 4.416 |

| Treeline Group | Transect ID | Start (UTM Easting) | Start (UTM Northing) | End (UTM Easting) | End (UTM Northing) | Azimuth (degrees) | Net Treeline Movement (m) | End Point Rate (m/y) | Confidence of Endpoint Rate (90%, m) | Linear Regression Rate (m/y) | Confidence of Linear Regression Rate (90%, m) |
|---|---|---|---|---|---|---|---|---|---|---|---|
| 15 | 182 | 484723.18 | 6611866.3 | 485610.43 | 6611405 | 117.47 | 169.33 | 2.97 | 0.075 | 2.93 | 4.412 |
| 15 | 183 | 484731.59 | 6611884.4 | 485628.22 | 6611441.6 | 116.28 | 187.64 | 3.29 | 0.075 | 3.22 | 8.467 |
| 15 | 184 | 484819.86 | 6611907.1 | 485623.71 | 6611312.3 | 126.5 | 131.2 | 2.3 | 0.075 | 2.22 | 9.007 |
| 15 | 185 | 484828.13 | 6611924.7 | 485794.96 | 6611669.3 | 104.8 | 146.56 | 2.57 | 0.075 | 2.48 | 10.095 |
| 15 | 186 | 484950.09 | 6612030.3 | 485208.02 | 6611064.2 | 165.05 | 130.67 | 2.29 | 0.075 | 2.31 | 2.575 |
| 15 | 190 | 484891.54 | 6612019.5 | 485308.01 | 6611110.4 | 155.39 | 182.66 | 3.2 | 0.075 | 3.2 | 0.658 |
| 16 | 94 | 484924.62 | 6612978.4 | 485922.11 | 6613049.2 | 85.94 | 711.78 | 12.47 | 0.075 | 12.52 | 6.992 |
| 16 | 95 | 484926.2 | 6612958.5 | 485926.15 | 6612967.7 | 89.47 | 663.98 | 11.63 | 0.075 | 11.77 | 16.897 |
| 16 | 96 | 484924.98 | 6612938.7 | 485912.87 | 6612783.5 | 98.93 | 617.91 | 10.82 | 0.075 | 10.7 | 14.551 |
| 16 | 98 | 484915.49 | 6612899.8 | 485902.56 | 6612739.5 | 99.23 | 618.45 | 10.83 | 0.075 | 10.7 | 15.537 |
| 16 | 100 | 484914.04 | 6612860.2 | 485911.07 | 6612783.1 | 94.42 | 628.72 | 11.01 | 0.075 | 10.87 | 17.071 |
| 16 | 101 | 484910.61 | 6612840.6 | 485906.01 | 6612744.8 | 95.5 | 624.24 | 10.93 | 0.075 | 10.74 | 24.15 |
| 16 | 103 | 484911.42 | 6612801.6 | 485905.79 | 6612695.6 | 96.08 | 612.99 | 10.74 | 0.075 | 10.78 | 4.981 |
| 16 | 104 | 484906.15 | 6612782.3 | 485821.98 | 6612380.7 | 113.68 | 587.49 | 10.29 | 0.075 | 10.37 | 10.301 |
| 17 | 199 | 484077.86 | 6612415.3 | 483510.63 | 6613238.8 | 325.44 | 205.75 | 3.6 | 0.075 | 3.68 | 9.088 |
| 17 | 200 | 484111.38 | 6612512.7 | 483575.39 | 6613356.9 | 327.59 | 273.05 | 4.78 | 0.075 | 4.83 | 5.633 |
| 17 | 201 | 484146.6 | 6612530.6 | 483452.72 | 6613250.7 | 316.06 | 206.82 | 3.62 | 0.075 | 3.58 | 5.475 |
| 17 | 202 | 484158.55 | 6612546.6 | 483415.97 | 6613216.4 | 312.05 | 207.1 | 3.63 | 0.075 | 3.6 | 2.856 |
| 17 | 203 | 484187.71 | 6612573.5 | 483414.65 | 6613207.9 | 309.37 | 188.42 | 3.3 | 0.075 | 3.25 | 5.679 |
| 17 | 204 | 484198.13 | 6612590.5 | 483394.71 | 6613185.9 | 306.54 | 192.02 | 3.36 | 0.075 | 3.32 | 5.289 |

| Treeline Group | Transect ID | Start (UTM Easting) | Start (UTM Northing) | End (UTM Easting) | End (UTM Northing) | Azimuth (degrees) | Net Treeline Movement (m) | End Point Rate (m/y) | Confidence of Endpoint Rate (90%, m) | Linear Regression Rate (m/y) | Confidence of Linear Regression Rate (90%, m) |
|---|---|---|---|---|---|---|---|---|---|---|---|
| 17 | 205 | 484306.1 | 6612610.7 | 483423.9 | 6613081.6 | 298.09 | 166.76 | 2.92 | 0.075 | 2.96 | 5.174 |
| 17 | 206 | 484211.26 | 6612605.3 | 483582.95 | 6613383.3 | 321.07 | 97.94 | 1.72 | 0.075 | 1.74 | 2.785 |
| 17 | 207 | 484292.54 | 6612660 | 483442.86 | 6613187.3 | 301.82 | 139.53 | 2.44 | 0.075 | 2.47 | 2.838 |
| 17 | 208 | 484292.54 | 6612660 | 483442.86 | 6613187.3 | 301.82 | 228.48 | 4 | 0.075 | 3.99 | 1.983 |
| 17 | 209 | 484146.6 | 6612530.6 | 483452.72 | 6613250.7 | 316.06 | 201.71 | 3.53 | 0.075 | 3.48 | 6.743 |

# Appendix B

Position, distance, and rate of change statistics for historic and current shrublines in the upper Chilkoot Unit of Klondike Gold Rush NHP.

| Shrubline Group | Trans. ID | Start (UTM Easting) | Start (UTM Northing) | End (UTM Easting) | End (UTM Northing) | Azimuth (degrees) | Net Shrubline Movement (m) | End Point Rate (m/y) | Confidence of Endpoint Rate (90%, m) | Linear Regression Rate (m/y) | Confidence of Linear Regression Rate (90%, m) |
|---|---|---|---|---|---|---|---|---|---|---|---|
| 1 | 3 | 485318.04 | 6614617.17 | 485412.78 | 6614585.17 | 108.66 | 27.14 | 0.49 | 0.06 | 0.55 | 4.533 |
| 1 | 4 | 485316.31 | 6614597.4 | 485416.3 | 6614597.24 | 90.09 | 42.41 | 0.77 | 0.06 | 0.81 | 3.108 |
| 1 | 5 | 485317.98 | 6614578.48 | 485417.11 | 6614565.32 | 97.56 | 23.21 | 0.42 | 0.06 | 0.41 | 1.292 |
| 1 | 6 | 485311.3 | 6614559.66 | 485408.75 | 6614537.22 | 102.97 | 29.06 | 0.53 | 0.06 | 0.56 | 2.353 |
| 1 | 7 | 485309.08 | 6614539.86 | 485403.36 | 6614506.51 | 109.48 | 27.83 | 0.51 | 0.06 | 0.52 | 1.151 |
| 1 | 8 | 485298.65 | 6614523.92 | 485392.66 | 6614489.82 | 109.94 | 40.02 | 0.73 | 0.06 | 0.74 | 1.152 |
| 1 | 9 | 485296.22 | 6614504.4 | 485391.78 | 6614474.93 | 107.14 | 57.61 | 1.05 | 0.06 | 1.05 | 0.258 |
| 1 | 10 | 485287.65 | 6614488.25 | 485381.29 | 6614453.13 | 110.56 | 35.87 | 0.65 | 0.06 | 0.63 | 2.221 |
| 1 | 11 | 485283.06 | 6614469.32 | 485382.27 | 6614456.76 | 97.22 | 23.27 | 0.42 | 0.06 | 0.39 | 2.824 |
| 1 | 12 | 485282.95 | 6614451.07 | 485382.01 | 6614437.43 | 97.84 | 35.98 | 0.65 | 0.06 | 0.67 | 0.923 |
| 1 | 69 | 485277.91 | 6614431.85 | 485377.5 | 6614422.84 | 95.17 | 14.55 | 0.26 | 0.06 | 0.26 | 0.625 |
| 2 | 16 | 485142.94 | 6614672.56 | 485140.57 | 6614772.53 | 358.64 | 28.22 | 0.51 | 0.06 | 0.54 | 2.141 |
| 2 | 17 | 485159.05 | 6614661.57 | 485192.05 | 6614755.97 | 19.27 | 29.11 | 0.53 | 0.06 | 0.54 | 0.684 |
| 2 | 18 | 485178.39 | 6614660.17 | 485204.15 | 6614756.79 | 14.93 | 32.09 | 0.58 | 0.06 | 0.59 | 0.454 |
| 2 | 19 | 485195.97 | 6614651.73 | 485232.43 | 6614744.84 | 21.38 | 41.33 | 0.75 | 0.06 | 0.76 | 0.743 |
| 2 | 20 | 485214.73 | 6614645.94 | 485241.74 | 6614742.22 | 15.67 | 37.58 | 0.68 | 0.06 | 0.68 | 0.088 |
| 2 | 21 | 485233.36 | 6614641.23 | 485282 | 6614728.61 | 29.11 | 32.8 | 0.6 | 0.06 | 0.59 | 0.68 |

| Shrubline Group | Trans. ID | Start (UTM Easting) | Start (UTM Northing) | End (UTM Easting) | End (UTM Northing) | Azimuth (degrees) | Net Shrubline Movement (m) | End Point Rate (m/y) | Confidence of Endpoint Rate (90%, m) | Linear Regression Rate (m/y) | Confidence of Linear Regression Rate (90%, m) |
|---|---|---|---|---|---|---|---|---|---|---|---|
| 2 | 23 | 485266.97 | 6614623.65 | 485253.55 | 6614722.74 | 352.28 | 47.74 | 0.87 | 0.06 | 0.88 | 1.105 |
| 2 | 25 | 485303.62 | 6614634.56 | 485266.28 | 6614727.33 | 338.07 | 28.48 | 0.52 | 0.06 | 0.51 | 0.735 |
| 2 | 76 | 485328.54 | 6614664.24 | 485238.38 | 6614707.5 | 295.64 | 19.3 | 0.35 | 0.06 | 0.33 | 1.817 |
| 2 | 83 | 485129.2 | 6614660.86 | 485087.77 | 6614751.87 | 335.53 | 17.95 | 0.33 | 0.06 | 0.34 | 0.75 |
| 3 | 29 | 485320.66 | 6614746.68 | 485347.85 | 6614842.92 | 15.78 | 26.51 | 0.48 | 0.06 | 0.48 | 0.215 |
| 3 | 85 | 485304.27 | 6614740.84 | 485270.7 | 6614835.04 | 340.39 | 6.44 | 0.12 | 0.06 | 0.11 | 0.227 |
| 4 | 30 | 485310.83 | 6614796.58 | 485320.04 | 6614896.16 | 5.29 | 50.94 | 0.93 | 0.06 | 0.94 | 1.436 |
| 4 | 31 | 485330.23 | 6614794.79 | 485350.92 | 6614892.63 | 11.94 | 59.88 | 1.09 | 0.06 | 1.12 | 2.168 |
| 5 | 34 | 485388.27 | 6615440.48 | 485400.23 | 6615341.2 | 173.13 | 22.23 | 0.4 | 0.06 | 0.42 | 0.912 |
| 5 | 35 | 485369.41 | 6615434.37 | 485426.86 | 6615352.53 | 144.93 | 47.05 | 0.86 | 0.06 | 0.87 | 1.092 |
| 5 | 37 | 485360.87 | 6615399.68 | 485460.43 | 6615409.08 | 84.61 | 14.72 | 0.27 | 0.06 | 0.26 | 0.561 |
| 5 | 38 | 485360.52 | 6615388.29 | 485432.8 | 6615319.18 | 133.71 | 41.23 | 0.75 | 0.06 | 0.75 | 0.32 |
| 6 | 42 | 485345.96 | 6615297.55 | 485436.24 | 6615254.56 | 115.46 | 22.19 | 0.4 | 0.06 | 0.4 | 0.612 |
| 6 | 43 | 485333.91 | 6615282.01 | 485423.43 | 6615237.45 | 116.46 | 28.06 | 0.51 | 0.06 | 0.52 | 1.163 |
| 6 | 44 | 485328.97 | 6615263.43 | 485418.05 | 6615217.98 | 117.03 | 26.31 | 0.48 | 0.06 | 0.48 | 0.05 |
| 6 | 45 | 485316.81 | 6615248.5 | 485402.57 | 6615197.08 | 120.95 | 21.32 | 0.39 | 0.06 | 0.37 | 1.169 |
| 7 | 46 | 485862.18 | 6616055.71 | 485962.16 | 6616053.82 | 91.08 | 52.04 | 0.95 | 0.06 | 0.92 | 2.28 |
| 7 | 47 | 485861.8 | 6616035.75 | 485961.46 | 6616043.92 | 85.31 | 53.38 | 0.97 | 0.06 | 0.97 | 0.352 |
| 7 | 49 | 485872.91 | 6615997.6 | 485961.38 | 6616044.21 | 62.22 | 43.86 | 0.8 | 0.06 | 0.79 | 0.823 |
| 7 | 50 | 485883.94 | 6615980.96 | 485961.3 | 6616044.34 | 50.67 | 92.02 | 1.67 | 0.06 | 1.68 | 0.399 |

| Shrubline Group | Trans. ID | Start (UTM Easting) | Start (UTM Northing) | End (UTM Easting) | End (UTM Northing) | Azimuth (degrees) | Net Shrubline Movement (m) | End Point Rate (m/y) | Confidence of Endpoint Rate (90%, m) | Linear Regression Rate (m/y) | Confidence of Linear Regression Rate (90%, m) |
|---|---|---|---|---|---|---|---|---|---|---|---|
| 7 | 51 | 485898.08 | 6615966.87 | 485962.33 | 6616043.5 | 39.98 | 101.16 | 1.84 | 0.06 | 1.78 | 4.725 |
| 8 | 52 | 485268.07 | 6616265.79 | 485357.27 | 6616310.98 | 63.13 | 51.91 | 0.94 | 0.06 | 0.92 | 2.332 |
| 8 | 53 | 485276.8 | 6616248.55 | 485374.06 | 6616271.82 | 76.55 | 63.35 | 1.15 | 0.06 | 1.15 | 0.12 |
| 8 | 54 | 485276.43 | 6616230.85 | 485365.57 | 6616185.52 | 116.95 | 34.72 | 0.63 | 0.06 | 0.64 | 0.512 |
| 8 | 55 | 485261.48 | 6616218.42 | 485343.3 | 6616160.93 | 125.09 | 44.81 | 0.81 | 0.06 | 0.82 | 0.78 |
| 9 | 91 | 485181.25 | 6616257.72 | 485271.69 | 6616215.05 | 115.26 | 9.47 | 0.17 | 0.06 | 0.18 | 0.262 |
| 9 | 92 | 485188.4 | 6616273.5 | 485276.66 | 6616320.51 | 61.96 | 26.17 | 0.48 | 0.06 | 0.46 | 1.367 |
| 9 | 93 | 485171.31 | 6616276.38 | 485187.92 | 6616374.99 | 9.56 | 16.16 | 0.29 | 0.06 | 0.3 | 0.423 |
| 10 | 61 | 485101.74 | 6615997.26 | 485067.72 | 6616091.29 | 340.11 | 79.95 | 1.45 | 0.06 | 1.45 | 0.498 |
| 10 | 62 | 485116.72 | 6616009.78 | 485039.34 | 6616073.11 | 309.3 | 84.68 | 1.54 | 0.06 | 1.54 | 0.14 |
| 10 | 63 | 485126.02 | 6616026.92 | 485070.95 | 6616110.39 | 326.58 | 47.74 | 0.87 | 0.06 | 0.83 | 3.234 |
| 10 | 94 | 485145.2 | 6616028.57 | 485111.19 | 6616122.61 | 340.12 | -2.89 | -0.05 | 0.06 | -0.07 | 1.471 |
| 10 | 95 | 485160.95 | 6616039.56 | 485083.87 | 6616103.25 | 309.57 | -2.53 | -0.05 | 0.06 | -0.06 | 0.929 |
| 10 | 96 | 485168.57 | 6616056.85 | 485095.15 | 6616124.74 | 312.76 | 3.5 | 0.06 | 0.06 | 0.06 | 0.019 |

The Department of the Interior protects and manages the nation’s natural resources and cultural heritage; provides scientific and other information about those resources; and honors its special responsibilities to American Indians, Alaska Natives, and affiliated Island Communities.

NPS 461/137324, March 2017

**National Park Service**
**U.S. Department of the Interior**

**Natural Resource Stewardship and Science**
1201 Oakridge Drive, Suite 150
Fort Collins, CO 80525

www.nature.nps.gov